AD-A142 143 A LABORATORY FACILITY FOR THE MEASUREMENT OF THE 1/1
OPTICAL PROPERTIES OF OBSCURANTS(U) ELECTRONICS
RESEARCH LAB ADELAIDE (AUSTRALIA) D J GAMBLING ET AL.
UNCLASSIFIED AUG 83 ERL-0287-TM F/G 17/8 NL

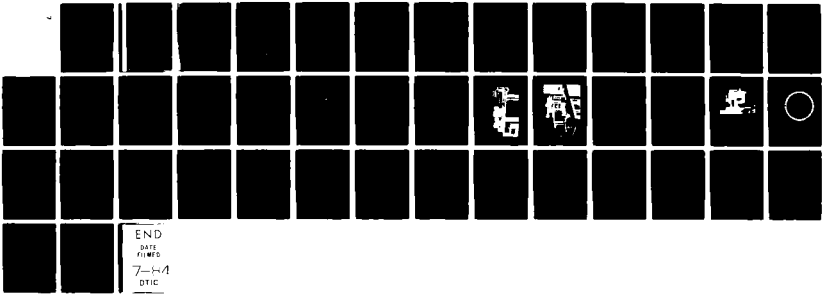

END
DATE FILMED
7-84
DTIC

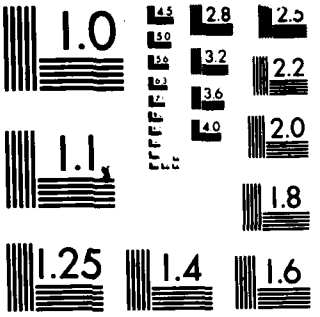

ERL-0287-TM

AR-003-697

AUSTRALIA

DEPARTMENT OF DEFENCE

DEFENCE SCIENCE AND TECHNOLOGY ORGANISATION

ELECTRONICS RESEARCH LABORATORY

DEFENCE RESEARCH CENTRE SALISBURY
SOUTH AUSTRALIA

TECHNICAL MEMORANDUM

ERL-0287-TM

A LABORATORY FACILITY FOR THE MEASUREMENT OF THE OPTICAL PROPERTIES OF OBSCURANTS

D.J. GAMBLING, F.R. DALE, O.S. SCOTT and J. BENTLEY *

* Materials Research Laboratories

Technical Memoranda are of a tentative nature, representing the views of the author(s), and do not necessarily carry the authority of the Laboratory.

COPY No. 25

Approved for Public Release

The official documents produced by the Laboratories of the Defence Research Centre Salisbury are issued in one of five categories: Reports, Technical Reports, Technical Memoranda, Manuals and Specifications. The purpose of the latter two categories is self-evident, with the other three categories being used for the following purposes:

Reports	:	documents prepared for managerial purposes.
Technical Reports	:	records of scientific and technical work of a permanent value intended for other scientists and technologists working in the field.
Technical Memoranda	:	intended primarily for disseminating information within the DSTO. They are usually tentative in nature and reflect the personal views of the author.

AR-003-697

DEPARTMENT OF DEFENCE

DEFENCE SCIENCE AND TECHNOLOGY ORGANISATION

ELECTRONICS RESEARCH LABORATORY

TECHNICAL MEMORANDUM

ERL-0287-TM

A LABORATORY FACILITY FOR THE MEASUREMENT OF THE OPTICAL PROPERTIES OF OBSCURANTS

D.J. Gambling, F.R. Dale, O.S. Scott and J. Bentley*

SUMMARY

The presence of natural and vehicle-made dusts, fires and smoke obscurants seriously degrades the performance of electro-optical sensors operated in military environments.

This memorandum describes a laboratory facility for the measurement of the visual and infrared mass extinction coefficients of obscurants under controlled environmental conditions.

* Materials Research Laboratories

POSTAL ADDRESS: Director, Electronics Research Laboratory,
Box 2151, GPO, Adelaide, South Australia, 5001.

TABLE OF CONTENTS

LIST OF FIGURES

1. INTRODUCTION

Military electro-optical sensors and missile guidance systems are generally employed in less than the optimum optical conditions. Thus there is a need to be able to predict their performance when operated in various environments.

Of particular interest to the present work are the optical extinction and emission effects of dust, both naturally-generated and man-made, urban, rural and vehicle fires, and man-made smoke obscurants. The spectral range of interest extends from the solar-blind ultraviolet (0.25 to 0.29 μm) through the visible (0.4 to 0.7 μm) to the long wave infrared (8 to 14 μm).

Several methods can be used to study the optical effects of obscurants. Field experiments indicate the effects that would be expected under actual military conditions; however they are costly, time-consuming, and are plagued by the unpredictable nature of the environment. Chamber experiments, on the other hand, can be controlled, are generally repeatable, and can be executed relatively quickly. Unfortunately, the results of chamber experiments cannot be easily extrapolated to field conditions, and can be considered as being representative only. Therefore it is generally concluded that both classes of experiment should be carried out in order to obtain a complete understanding of the properties of smoke obscurants.

This memorandum describes a laboratory facility for the measurement of the visual and infrared mass extinction coefficients of obscurants under controlled environmental conditions. The facility was developed as a result of co-operation between the Electronics Research Laboratory (ERL) and the Materials Research Laboratories (MRL).

MRL was responsible for the construction of the smoke chamber, ERL for the design and development of the optical transmissometer equipment and data-logging system(ref.1). The equipment is based at MRL and operated by MRL staff.

2. DEFINITIONS OF PERTINENT OPTICAL PARAMETERS

According to the Beer-Lambert relationship, radiation of intensity, I_λ, at wavelength, λ, transmitted through a homogeneous optically thin medium over a distance, s, is attenuated follows:

$$\frac{dI_\lambda}{ds} = -\delta I_\lambda \qquad (1)$$

where δ is the attenuation coefficient (m^{-1}). The significance of the optically thin medium is that the single scattering mechanism predominates.

The attenuation coefficient can be rewritten in terms of more physically-realisable quantities thus:

$$\delta = \alpha C \qquad (2)$$

where:

α = mass extinction coefficient ($m^2\ g^{-1}$)

C = aerosol mass concentration ($g\ m^{-3}$)

Therefore:

$$\frac{dI_\lambda}{ds} = -\alpha C I_\lambda \tag{3}$$

so that

$$\ln(I_\lambda / I_{o\lambda}) = -\alpha Cs \tag{4}$$

and

$$\alpha = \frac{-\ln(I_\lambda / I_{o\lambda})}{Cs} \tag{5}$$

In the case of the smoke chamber measurements, $I_{o\lambda}$ and I_λ are the measured signals without smoke and with smoke, respectively, for a given wavelength, s is the optical path length, and C is determined by drawing a known volume of aerosol through a Millipore filter and determining the mass of particulate deposited on the filter. For hygroscopic smoke particles such as red and white phosphorus, which absorb atmospheric water vapour, the mass of smoke material is given by the mass of the original smoke material multiplied by the mass yield factor as a result of the additional water absorbed. As an example, the mass yield factor for red phosphorus is given in the following table.

Mass yield factor for red phosphorus	
RELATIVE HUMIDITY	MASS YIELD FACTOR
40	5
60	6
80	9.3
9[illegible]	16.3

Using equation (5), it is possible to derive a design goal for an obscurant in field conditions on the basis of a desired transmission. For example, if it is required to reduce the transmission to 0.1, then it can be shown using equation (5) that:

$$\alpha = \frac{2.3}{Cs} m^2 \ g^{-1}$$

Assuming a cylindrically-shaped cloud of 10 m diameter and length 100 m, produced from 500 gm of material (including atmospheric water vapour) it then follows that $\alpha \sim 3.6 \ m^2 \ g^{-1}$ across the diameter.

3. THE SMOKE CHAMBER

A test chamber was constructed at MRL with a volume of 35 cubic metres (4.8 m x 2.8 m x 2.6 m). A sketch of the chamber is shown in figure 1.

The chamber consists of a wooden frame lined with fibro cement sheeting. Ports have been provided at both ends and sides and are approximately one metre from the floor. Four small tangential fans are situated on the floor in each corner to ensure uniform dispersal of aerosols and particulate materials. An extraction fan and flue are situated at the top of the chamber for exhausting after each test.

Particulate materials are injected through a side port using a high pressure spray gun and aerosols such as red phosphorus, oleum and HC smoke are generated by burning the appropriate materials or, in the case of oleum, volatilizing it using a gas burner. The weight of smoke material used is noted, and entered into the computer for automatic calculation of the concentration in the chamber.

4. THE OPTICAL TRANSMISSOMETER EQUIPMENT

4.1 Factors affecting the design of the equipment

The primary design aims for the optical transmissometer equipment were high sensitivity, wide spectral bandwidth, simplicity and reliability. As the former two aims conflicted with the latter, a compromise in performance had to be made; these aspects are discussed in the next section.

4.1.1 Choice of detectors

The initial transmissometer equipment configuration covers the bandwidth from the visible to the far infrared by means of two separate transmissometers. The visible and near IR transmissometer covers the bandwidth from 0.4 to 1.1 μm, which is primarily determined by the spectral responsivity of the silicon detector. The infrared transmissometer covers the 2.5 to 14.5 μm bandwidth, which is primarily determined by the coverage of a standard circular variable filter set. A Golay cell was chosen as the infrared detector because of its simplicity of operation, the wide spectral bandwidth, and its room temperature operation. The disadvantage of the Golay cell are its low detectivity (D*) and frequency response, and its susceptibility to vibration.

4.1.2 Receiver field of view

Errors in the measurement of transmission can occur due to the finite beamwidth of the receiver, as the Beer-Lambert relationship (equation (1)) is only applicable to the direct beam. Thus as the receiver beamwidth is increased, so is the error in measured transmission due to single and multiple scattered radiation, which is scattered into the receiver by off-axis particles. The magnitude of this effect is dependent upon the size and type of scattering particles.

Estimates of the effects of the receiver beamwidth are given in figure 2(ref.1) which shows a correction factor to be applied to measured laser beam intensities through three different cloud types as a function of a parameter which includes the source wavelength, cloud particle mode radius and receiver field of view. As the smoke chamber particulates are similar in size distribution to the type C (large particle) cloud, the abscissa parameter in figure 2 could be as high as 0.9 and yet maintain the measured error to less than 10%. For a cloud mode radius of 4 μm this is equivalent to the following receiver fields of view:

VISIBLE/NIR (0.4 to 1.1 μm)	MID/FIR (2.5 to 14.5 μm)
< 0.0022 rad (1.2°)	< 0.288 rad (16.5°)

It should be noted that errors in measured signals arising from multiple scattering effects are systematic, and can be corrected by a simple wavelength - dependent formula as shown in figure 2.

4.1.3 The environment

Consideration was given in the design to the effects of the dirty and corrosive environment in which the optical equipment would operate. All optics are separated from the chamber environment by a thin membrane of polyethylene ('Gladwrap'), 0.013 mm thick. Furthermore, a curtain of clean air is blown over the polyethylene windows to minimise the deposition of particulates and corrosive materials. The infrared receiver is housed in an airtight container maintained at a positive pressure with dry nitrogen.

4.2 Basic layout of the transmissometer equipment

Figure 3 shows the basic layout of the transmissometer equipment. The sources (figure 4) are situated at one end of the smoke chamber; the receivers (figure 5) are located at the other end of the 4.8 m path.

4.3 Visible/NIR transmissometer

A schematic diagram of the visible/NIR transmissometer is shown in figure 6. The source and receiver systems are shown in figures 4 and 5 respectively. Their characteristics are as follows:

Source: 100 W quartz iodide lamp at the focus of an f/0.75 pyrex aspheric lens, 33 mm clear aperture. The lamp is powered by an Oriel d.c. power supply. The source is chopped at a frequency of 120 Hz.

Receiver: YAG 100 silicon photodiode at the focus of a plano-convex glass lens, f/4, 32 mm clear aperture. A field stop of diameter 0.89 mm limits the field of view of the receiver to 0.38°.

A 10-position filter wheel is located prior to the detector and is rotated at a rate of one position per second. The following filters are presently incorporated:

(i) spectral response matched to the eye;

(ii) narrow band centred on 0.72 μm, bandwidth 0.035 μm;

(iii) narrow band centred on 1.06 μm, bandwidth 0.009 μm.

4.4 IR transmissometer

A schematic diagram of the IR transmissometer system is shown in figure 7. The source and receiver systems are shown in figures 4 and 5. Their characteristics are as follows:

Source: A Nernst glower is located at the focus of an f/0.8 Germanium lens with a 33 mm clear aperture. The source is chopped in synchronism with the optical pick-off on the filter wheel (see below).

The chopper shown in figure 7 is a modified loudspeaker. An extension has been fixed to the moving coil so that the infrared source is blanked by the extension for a fixed interval in synchronism with each pulse from the optical pick-off. The samples recorded by the computing system are taken immediately prior to source blanking. The side of the coil extension facing the chamber is gold plated so that the infrared radiation is minimised when the source is blanked.

The Nernst glower is powered by a constant current power supply operating at 0.6 A. In order to minimise damage to the glower, it is powered continuously; when not in operation, the glower is run with a stand-by current of 0.2 A. As the refractory material of the glower has a high resistance at room temperature, and a negative temperature coefficient, it is started by a heater coil adjacent to the glower. The heater coil automatically switches off when the glower achieves a threshold of 0.18 A.

Receiver: An f/5 Germanium lens with a 25 mm clear aperture focusses radiation on to a slit, 1.2 mm wide. A circular variable interference filter (OCLI CV 2.5/14.5) covering the 2.5 to 14.5 μm spectral region in three discrete segments is located immediately behind the slit. The characteristics of the three filter segments are given in the following table:

SEGMENT	WAVELENGTH COVERAGE (μm)	HALF BANDWIDTH (% of wavelength)
1	2.475 - 4.471	<1.0%
2	4.333 - 8.043	<1.0%
3	8.093 - 14.675	<1.4%

The interference filter is rotated at a rate of 1.8 r/min; this is primarily limited by the time response of the Golay cell. It should be noted that the system spectral bandwidth is twice that given above because it was necessary to widen the slit to keep the received signal sufficiently large.

A circular ruled scale (figure 9) is located on the circular variable filter mount, with 100 divisions for each filter segment, which corresponds to the maximum spectral resolution of the interference filters. A reflecting optical transmit/receiver system (pick-up) reads the presence of each scale division and provides an electrical pulse which is used to provide a wavelength calibration for the filter system. The circular ruled scale was designed for the automatic data logging facility, which accepts all 100 data points per filter segment.

The wavelength scale was calibrated by inserting thin films of materials of known characteristics in the infrared beam in the chamber. Figures 10(a) and 10(b) are plots of the transmission of a polystyrene film as a function of wavelength. Figure 10(a) is the plot obtained from the smoke chamber measurements and figure 10(b) the characteristic provided by the suppliers of the film and measured on an infrared spectrometer.

The filtered radiation is focussed by a secondary Germanium lens onto a Golay cell (KRS-5 window). The Germanium lenses in both the source and receiver optics are coated with anti-reflection layers covering the 2.5 to 14.5 wavebana to minimise losses.

4.5 Operating System

The LSI 11/03 computer system which has been configured for data logging and analysis is described in reference 2. A block diagram of the system is shown in figure 11.

The computer, display unit, printer and plotter are located near the smoke chamber in a clean room, and most of the operations can be controlled from this room.

A pen recorder also located in the clean room provides a real-time plot of the infrared system signal on one channel. This was used in the development stages to ensure that the correct signal inputs were being measured, and for initial data analysis prior to installation of the data-logging system.

4.6 Infrared Data recording

Three sets of data are required for calculating the attenuation characteristics of a smoke. These are the 300 data values:

(a) with the source blanked (ie 'background' set, B_λ)

(b) with the source unblanked but no smoke in the chamber (ie a 'no smoke' set, $I_{o\lambda}$); and

(c) with the source unblanked and with smoke dispersed in the chamber (ie a 'smoke' set, I_λ).

All the operations except blanking the source and dispersing the smoke are controlled from the clean room. The origins of the background signals are radiation and reflection from the walls of the chamber at ambient

temperature, and radiation and reflection from the side of the filter and filter mount facing the detector which change as the mount rotates. It has been found that the background data changes with time after the filter motor is switched on. When approximtely twenty minutes have elapsed, background data is closely repeatable from revolution to revolution.

It is recommended that the 'background' 'no smoke' and 'smoke' data are recorded as close as possible in time and after twenty minutes of switch-on so that errors caused by background variations are minimised.

The procedure is controlled by the operator who is presented with a menu by the computing system.

The operator can choose:-

No Smoke Measurement
Background Measurement
Smoke Measurement
Calculate Data
Graph Results
Tabulate Results
Replot or Retabulate Previous Disc-Stored Data
Close down computer for the day

There are also procedures for installing diskettes and allocating run numbers.

On choosing a program from this menu the operator is prompted to enter the appropriate information and commands at the keyboard. For example, prior to a smoke measurement the operator is prompted to enter the smoke type, the chamber temperature and humidity and the number of filter revolutions to be used to provide an average set of data. The number of revolutions can be from 1 to 7. The 'background' and 'no-smoke' data are more accurate when averaged over 7 revolutions to reduce the effects of system noise, but because smoke particles can settle or otherwise change with time, the smoke data can be more accurate when taken during one revolution only.

On choosing to graph results, the operator is prompted to ensure that the paper and pen are ready and that the plotter is active. Sample plots of raw data, smoke transmission and extinction coefficient are shown in figures 12, 13 and 14. Using the DMP-4 plotter at present incorporated each plot takes about 3 min.

4.7 Visible Waveband Data Recording

A second channel of the pen recorder is used to provide a record of the visual waveband transmissometer outputs. The pen deflection for each of the filters is noted during both 'smoke' and 'no-smoke' runs, and the ratio of the two is the transmission. These ratios are plotted by hand at the appropriate wavelength values on the graphs containing the curves of transmission obtained automatically for the infrared region.

5. ERROR ANALYSIS

5.1 Errors in the IR mass extinction coefficient

Inherent in all the detected signals is a constant random noise component due to the detector noise. An A/D converter in the data logger would also inject a measurable noise component. As the received signals from the

mid/far IR receiver vary markedly throughout the spectrum due to the strong atmospheric and polyethylene absorption lines, the corresponding relative errors will vary accordingly.

If δ is the standard deviation of the total random noise, then the relative errors in each of the measured signals with clear air ($I_{o\lambda}$) and with smoke (I_λ) are $\delta/I_{o\lambda}$ and δ/I_λ respectively. The relative error in the ratio $I_\lambda/I_{o\lambda}$ is then:

$$\epsilon = \sqrt{\frac{\delta^2}{I_{o\lambda}^2} + \frac{\delta^2}{I_\lambda^2}} \tag{6}$$

and the measured extinction coefficient is then:

$$a + \Delta a = \frac{-\ln\left(\frac{I_\lambda}{I_{o\lambda}} + \epsilon \frac{I_\lambda}{I_{o\lambda}}\right)}{Cs} \tag{7}$$

Subtracting equation (5) from equation (7), it can be shown that:

$$\Delta a = \frac{-\ln(1 + \epsilon)}{Cs} \tag{8}$$

Therefore the relative error in the mass extinction coefficient is:

$$\frac{\Delta a}{a} = \frac{-\ln(1 + \epsilon)}{\ln(I_\lambda/I_{o\lambda})} \tag{9}$$

The random detector noise component was estimated to have a standard deviation of 0.0008 V. An estimate of the errors in the chart records (ignoring A/D conversion errors) was made by substituting this value for δ in equation (9) to compute $\Delta\alpha/\alpha$ for a range of values of $I_{o\lambda}$ and I_λ, the received signals being within the range 0 to 1.0 V. The results are shown in figure 15, which gives contours of equal error in α (in %) as a function of $I_{o\lambda}$ and I_λ.

It is evident from figure 15 that for a given clear air signal, I_o, there is an optimum value of I_λ to achieve a minimum error in extinction coefficient, α. High values of I_λ with respect to $I_{o\lambda}$ result in a high transmission of the obscurant, which gives a low value of α. Small errors in $I_{o\lambda}$ and I_λ therefore result in large errors in α. Similarly, for low values of I_λ with respect to $I_{o\lambda}$ (low transmission of the obscurant) the random error component is proportionally large, causing large errors in the estimate of α.

In figure 15, the optimum values of $I_{o\lambda}$ and I_{λ} are shown by the straight line, which has the equation as follows:

$$\log I_{\lambda} = m \log I_{o\lambda} + \log k$$

where m is the slope of the line and the constant, $k = I_{\lambda}$ when $I_{o\lambda} = 1.0$. Therefore, from the graph, $k = 0.3$, $m = 1$ and

$$\frac{I_{\lambda}}{I_{o\lambda}} = \text{transmission of obscurant} = k = 0.3.$$

Thus it follows that the smoke chamber experiments should be arranged such that the transmission of the obscurant is close to 0.3 in order to minimise the errors in the derived extinction coefficient.

Figure 15 was used to derive the permissible values of $I_{o\lambda}$ and I_{λ} to maintain the errors in derived extinction coefficient to less than 10%. The permissible region is shown in figure 16. It is evident that for a s.d. of 0.0008 V, the clear air signal should be no less than 0.025 V to maintain the errors in α to within 10%.

6. SAMPLE RESULTS

Plots can be produced of 'raw data' 'transmission' or 'extinction coefficient'. The raw data plot displays the 'no-smoke', and 'smoke' data as functions of wavelength. The 'no-smoke' plot is of course the combined characteristic of the source, atmosphere, detector and window material plus any background signal. The 'smoke' plot is the same as the 'no-smoke' plot but with reduced values in wavelengths regions where the smoke attenuates. A sample 'raw data' plot is shown in figure 12.

The 'no-smoke' graph has several notable features, determined by the combined interactions of the source spectral characteristics, the atmospheric absorption bands and the spectral characteristics of the polyethylene windows.

They include:

3.5 μm	polyethylene window absorption band
4.27 μm	CO_2 absorption peak
5.90 μm	H_2O absorption peak
6.25 μm	H_2O transmission peak
6.60 μm	H_2O absorption peak

The transmission plot is the ratio:

$$\frac{I_{\lambda} - B_{\lambda}}{I_{o\lambda} - B_{\lambda}}$$

plotted against wavelength (λ). A sample transmission plot is shown in figure 13.

The extinction coefficient can be plotted against wavelength as shown in figure 14. Equation (5) is modified to eliminate the effect of any background signals ie:

$$\alpha = \frac{-\ln\left[(I_\lambda - B_\lambda)/(I_{o\lambda} - B_\lambda)\right]}{Cs} \qquad (12)$$

The accuracy of α is calculated automatically using a modified equation 9:-

$$\frac{\Delta\alpha}{\alpha} = \frac{-\ln(1+\epsilon)}{\ln\left[(I_\lambda - B_\lambda)/(I_{o\lambda} - B_\lambda)\right]} \qquad (13)$$

In wavelength regions where this relative error is greater than 10% the values of α are omitted from the plot.

Figures 17, 18 and 19 show graphs of mass extinction coefficient versus wavelength for red phosphorus, hexochloroethane and oleum under similar conditions. They are characterised by:

(a) high mass extinction coefficients in the visible and near IR spectral regions; and

(b) low mass extinction coefficients in the mid and far IR regions.

Red phosphorus exhibits weak absorption bands in the 3 to 5 μm and 9 to 12 μm wavebands.

It is clear that the mass extinction coefficients in the mid and far IR wavebands, typically less than 1 m^2/g, fall far short of the design goal of 3.6 m^2/g for all three materials. Further investigations are now being undertaken to examine other materials for their potential as infrared screening agents.

7. CONCLUSIONS

A laboratory facility for the measurement of the visual and infrared mass extinction coefficients of obscurants under controlled environmental conditions has been developed. The equipment covers the spectral range from visible wavelengths (0.4 to 0.7 μm) to far infrared wavelengths (14 μm).

The equipment has been shown to perform satisfactorily. The automatic data acquisition system, which enables graphical results to be displayed immediately after each run, is also complete.

The mass extinction coefficients of three smokes which provide good attenuation in the visible region have been measured using the facility. The values obtained in the 3 to 5 and 8 to 14 μm bands were typically 1 m^2/g. Such values are below the design goal of 3.6 m^2/g, and other materials should be investigated.

8. ACKNOWLEDGEMENTS

Messrs J. Hicks and P. Mitchell assisted with the design of the optical and mechanical systems; Mrs J. Newgrain carried out the computer calculations. Mr J. Ingram interfaced the optical system with the data-logging system.

REFERENCES

No.	Author	Title
1	Ingram, J.D.	"A Data Logging System for the MRL Smoke Chamber". ERL Special Document ERL-0250-50 September 1982
2	Spencer, S. and Masinskas, J.	"Improving the Analysis of Spectral Transmission Records by using a Microprocessor Controlled Digitiser". MRL Technical Note No. 465
3	Holst, G.C.	"Infrared Transmission Through Screening Smokes: Experimental Considerations". Technical Report ARCSL-TR-80004, May 1980. Chemical Systems Laboratory, Aberdeen Proving Ground, Maryland

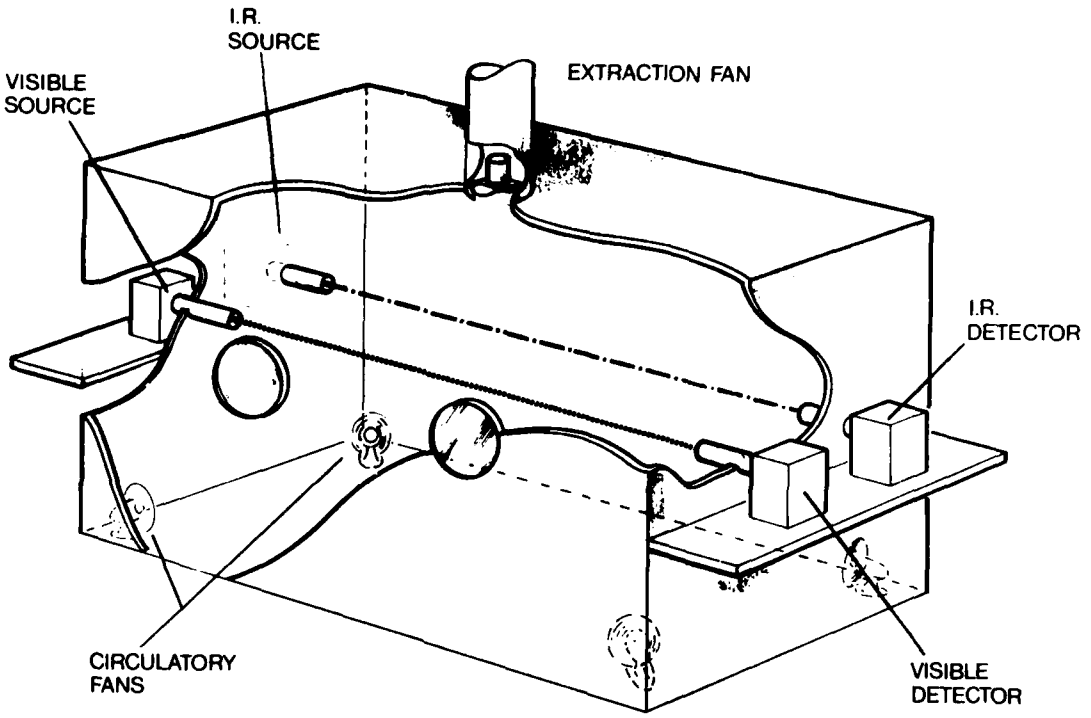

Figure 1. MRL smoke chamber

ERL-0287-TM
Figure 2

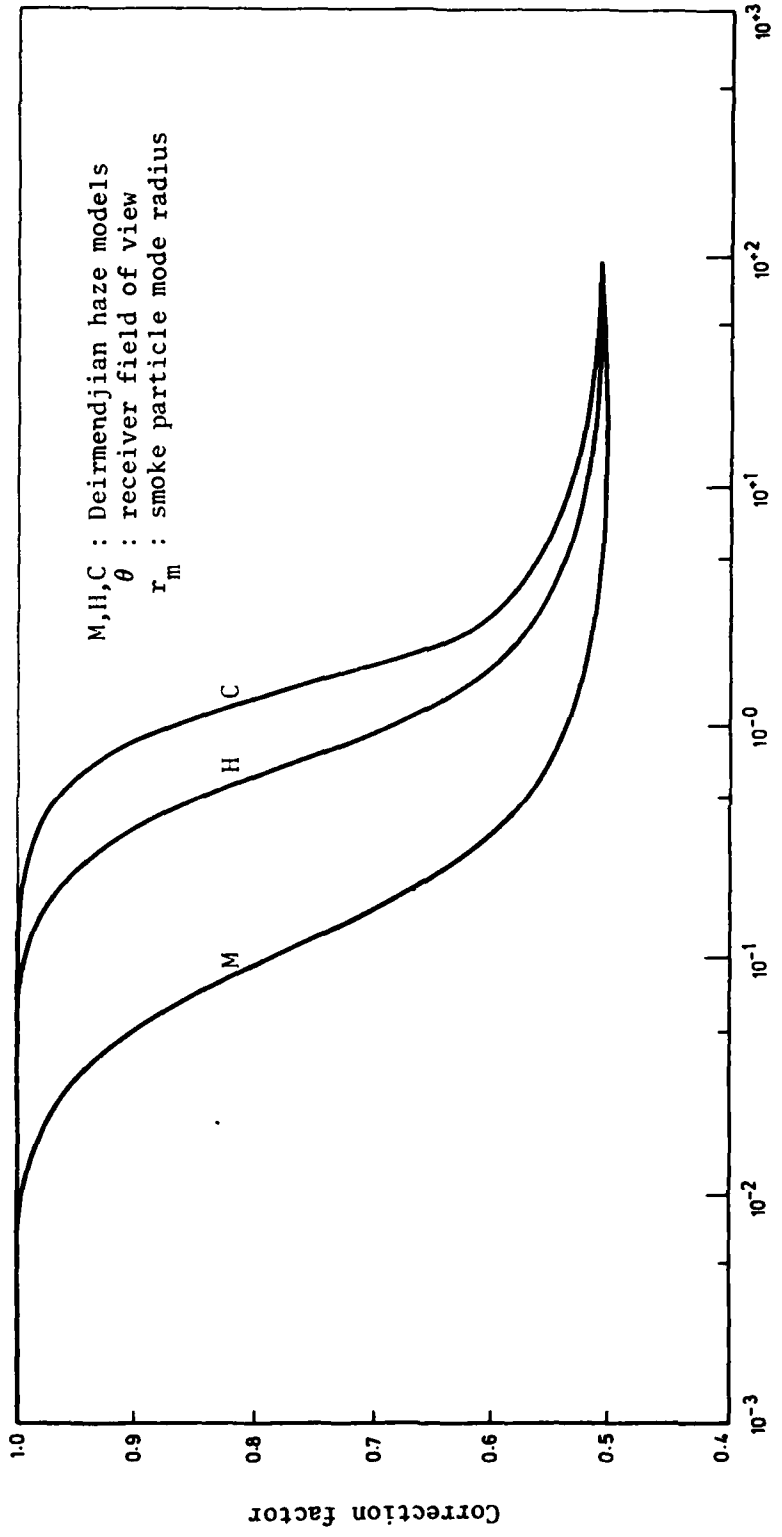

Figure 2. Correction to be applied to measured extinction coefficients

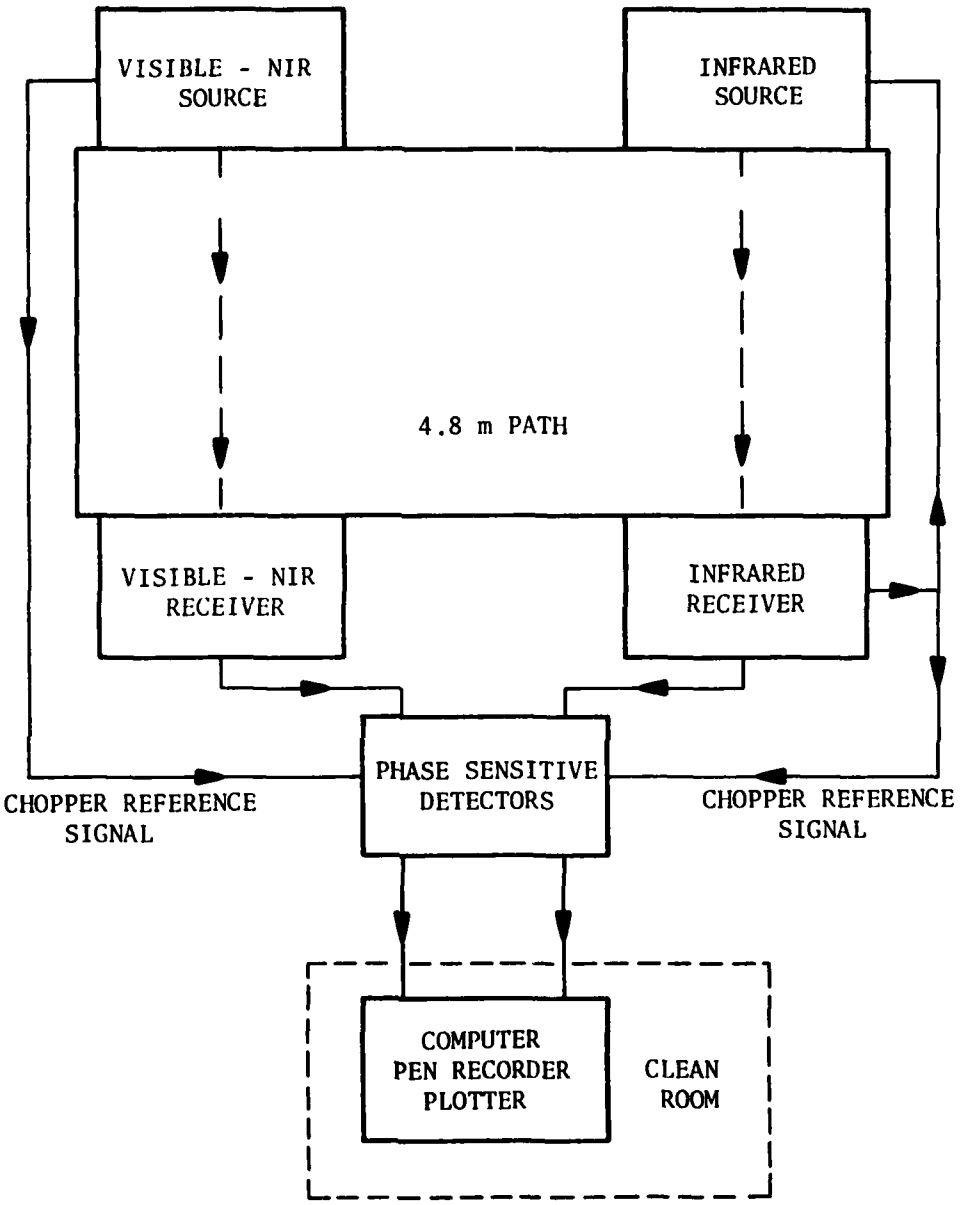

Figure 3. Basic layout of transmissometer system

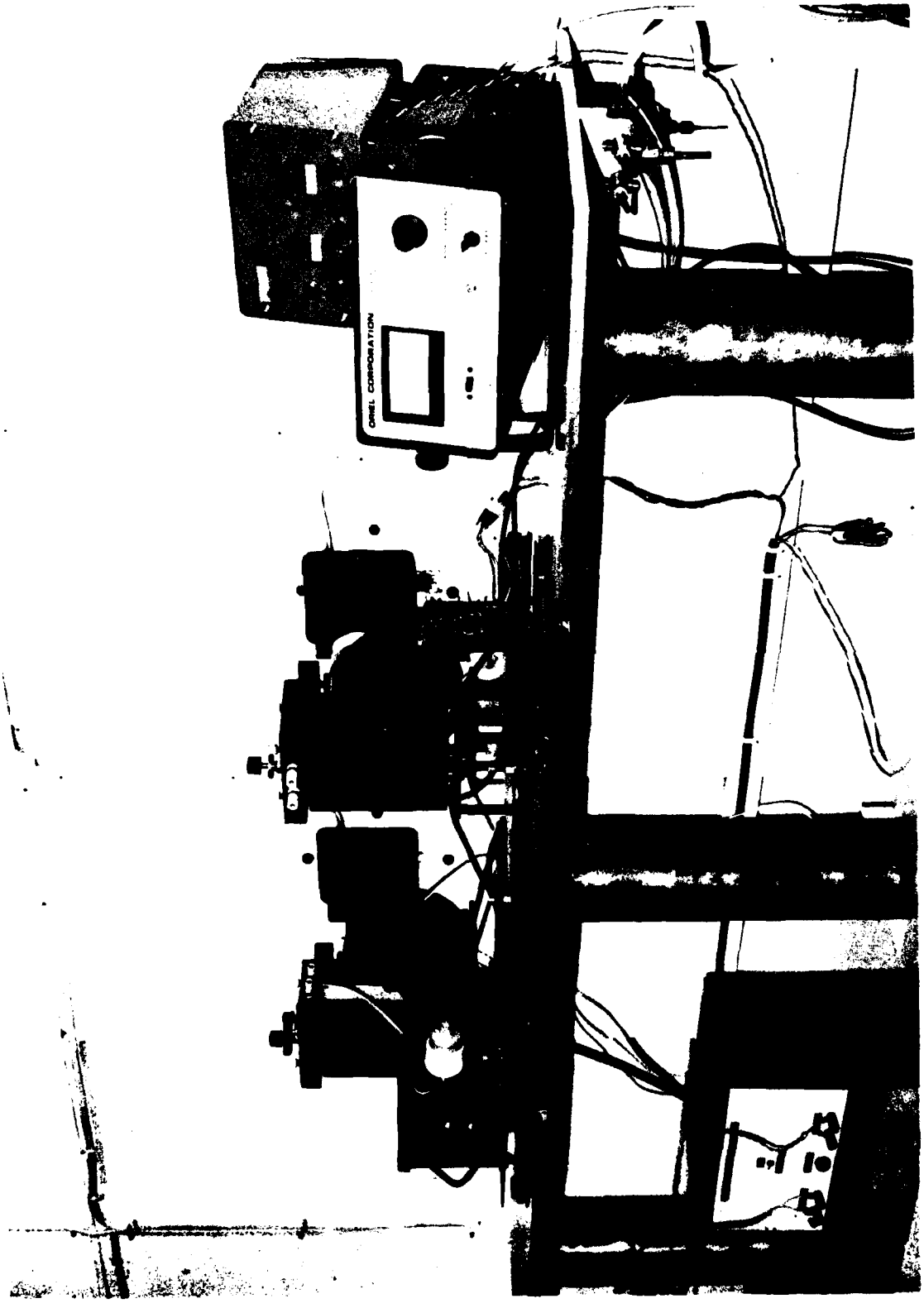

Figure 4. Infrared and visible/NIR transmitters

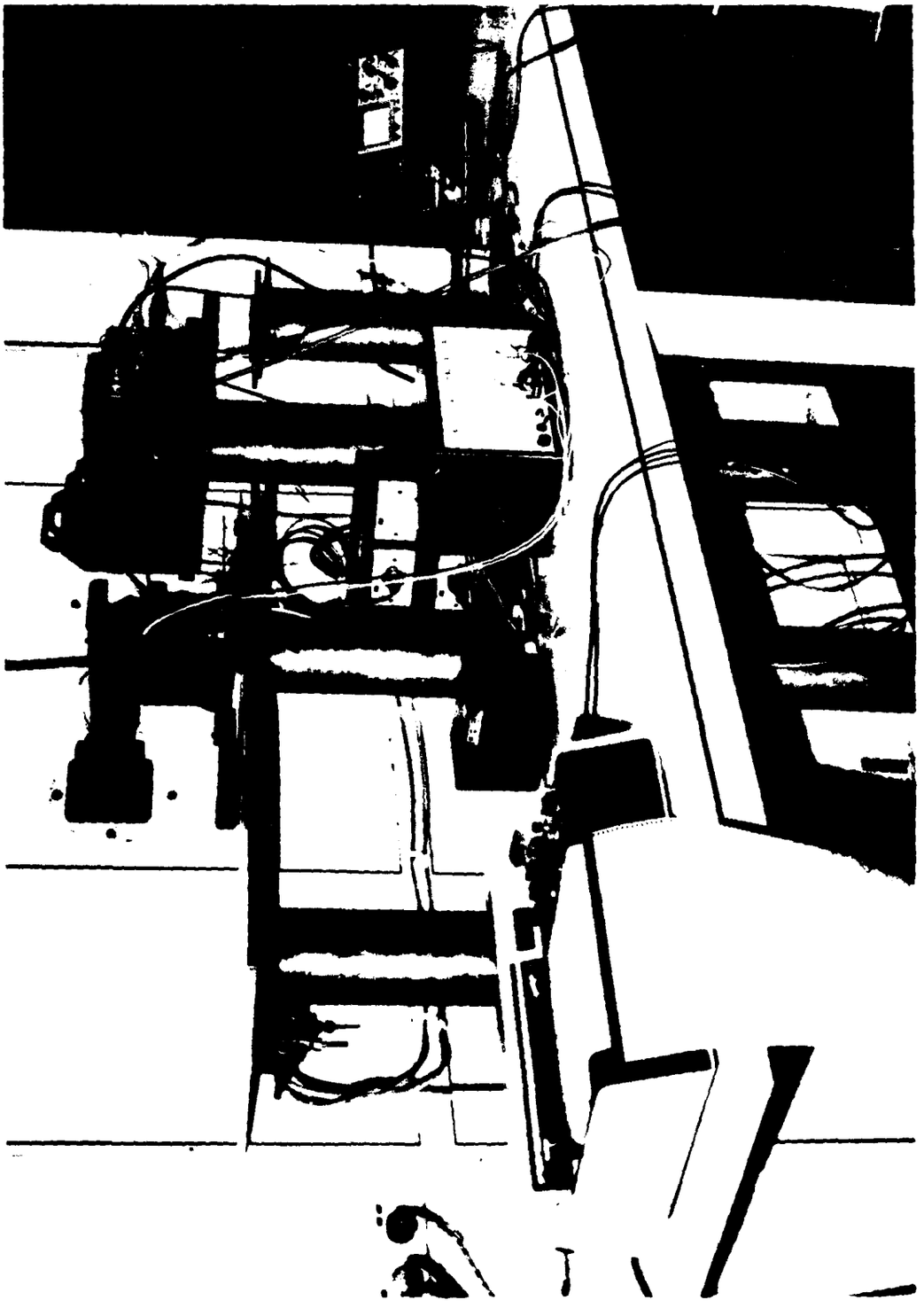

Figure 5. Infrared and visibile/NIR receivers

ERL-0287-TM
Figure 6

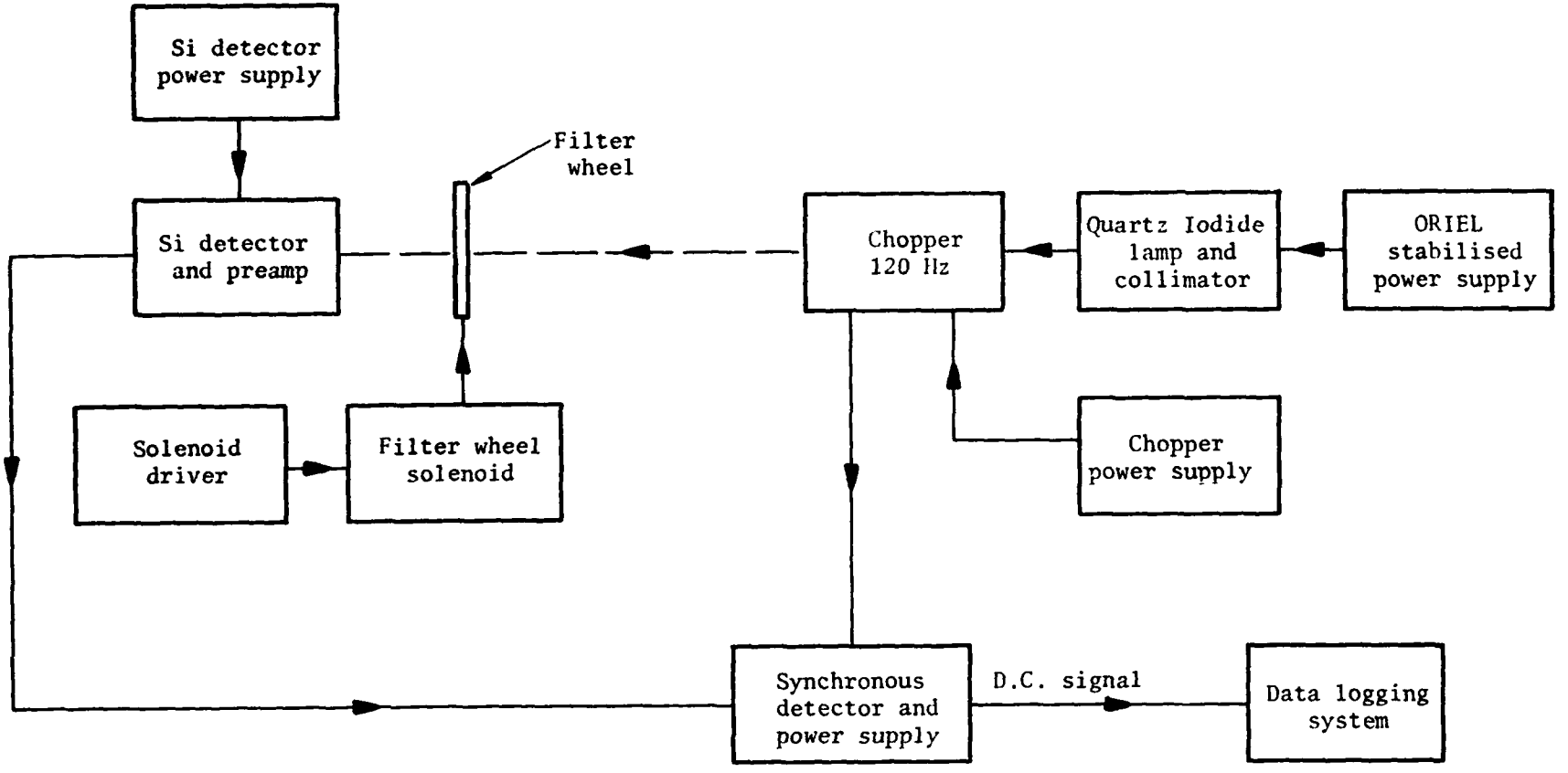

Figure 6. Schematic diagram of visible/NIR transmissometer system

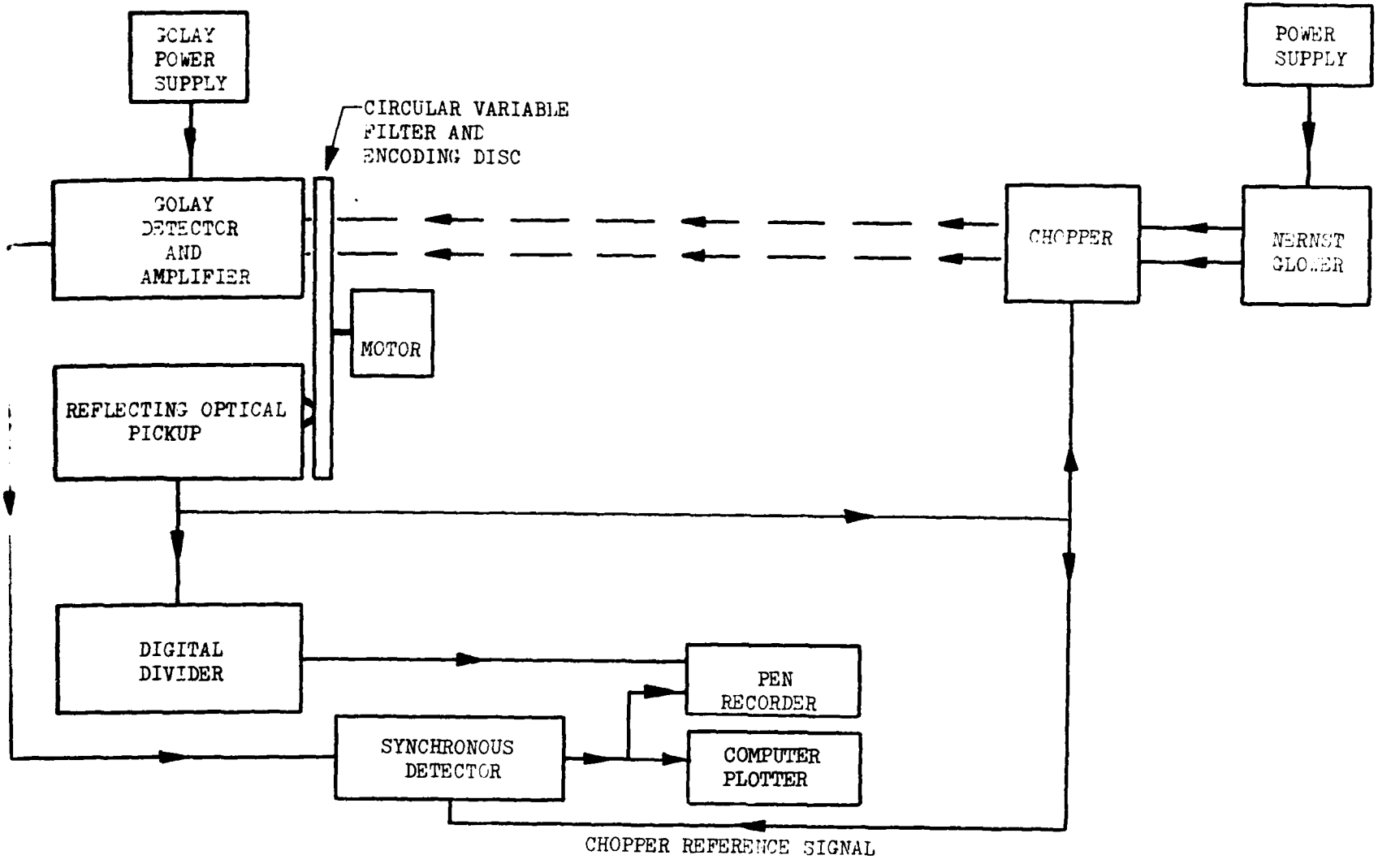

Figure 7. Schematic diagram of the IR transmissometer system

FRL-0287-TM
Figure 7

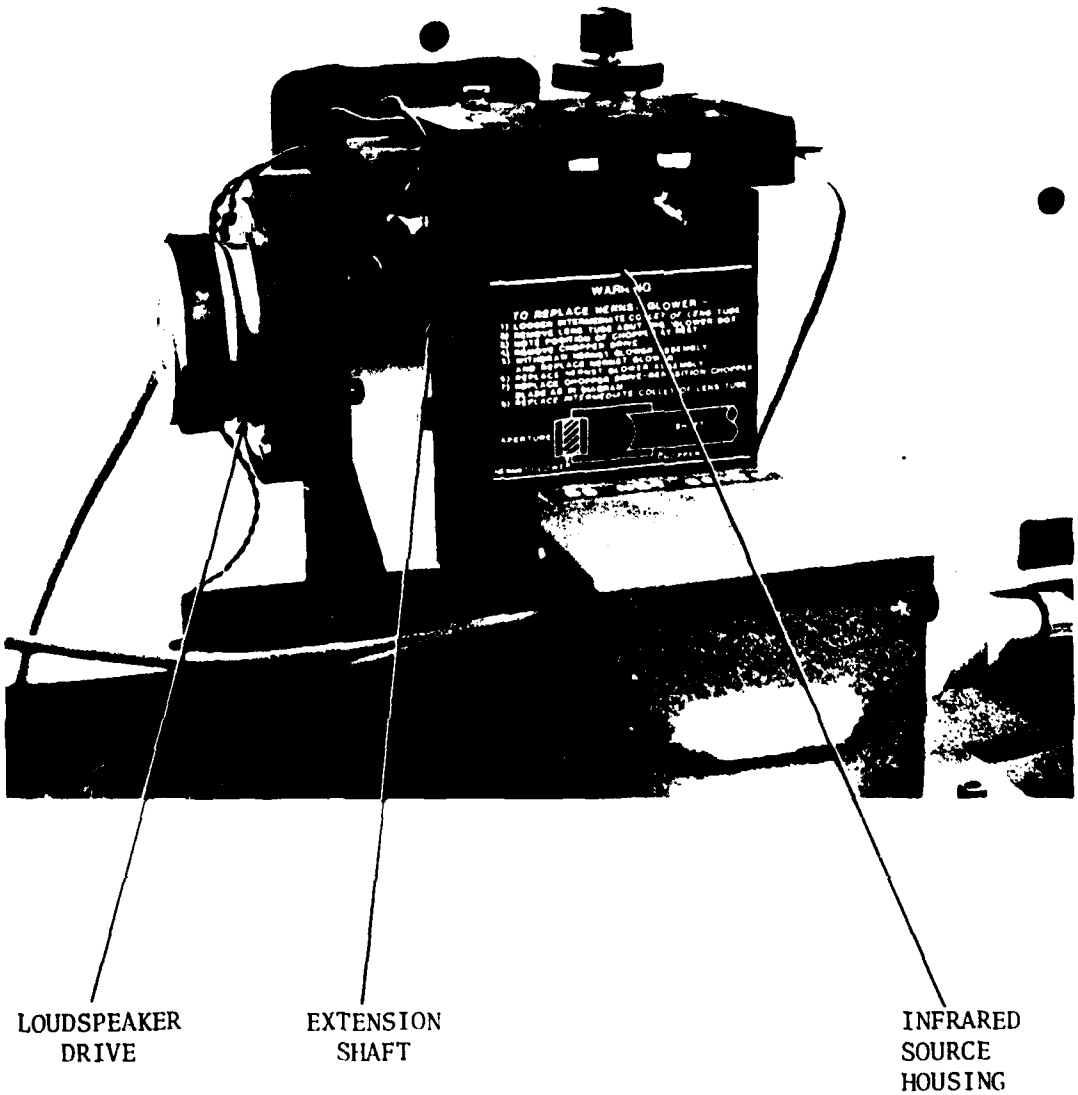

Figure 8. Chopper for infrared source

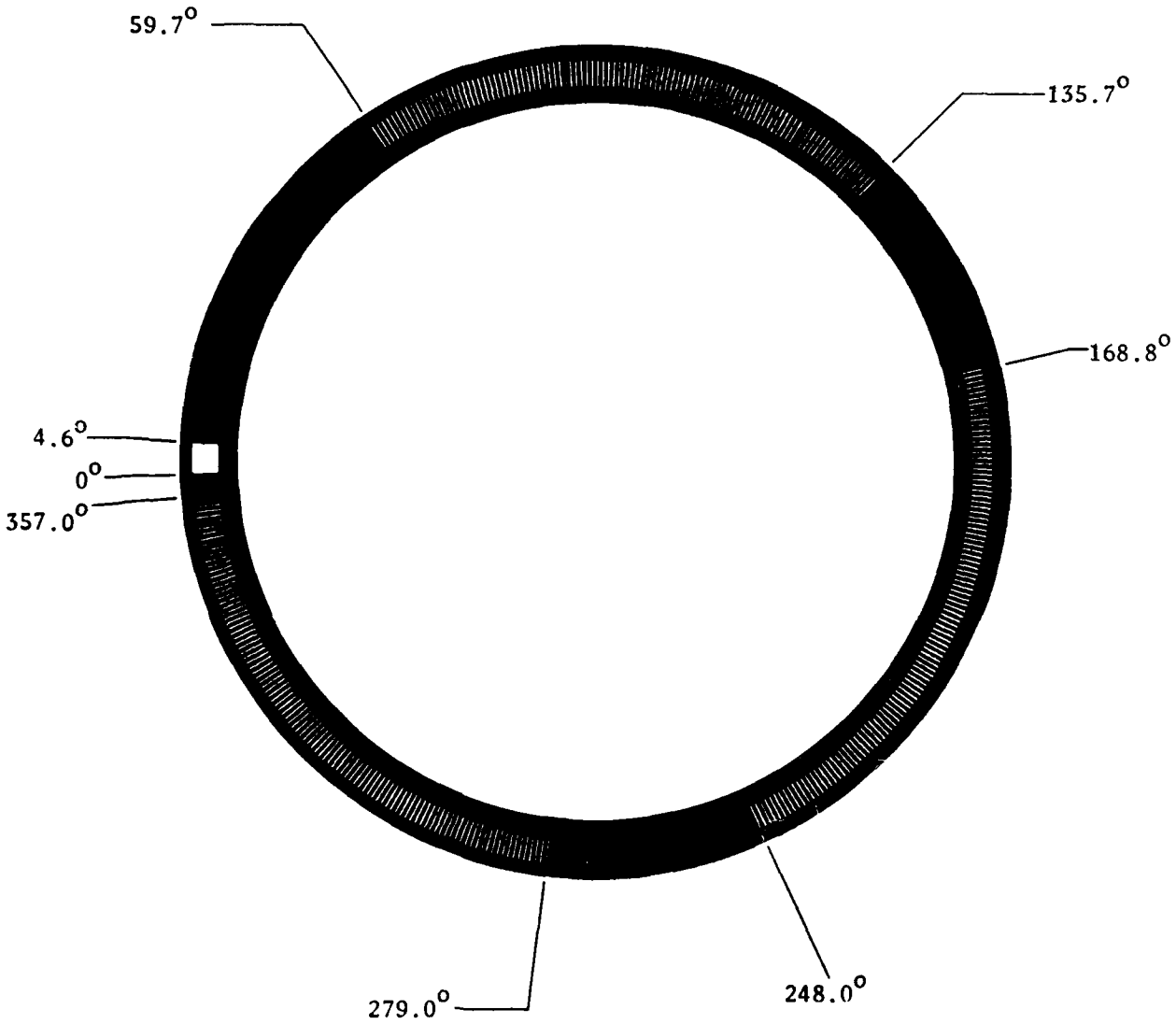

Figure 9. Circular graduated encoder disc for IR receiver

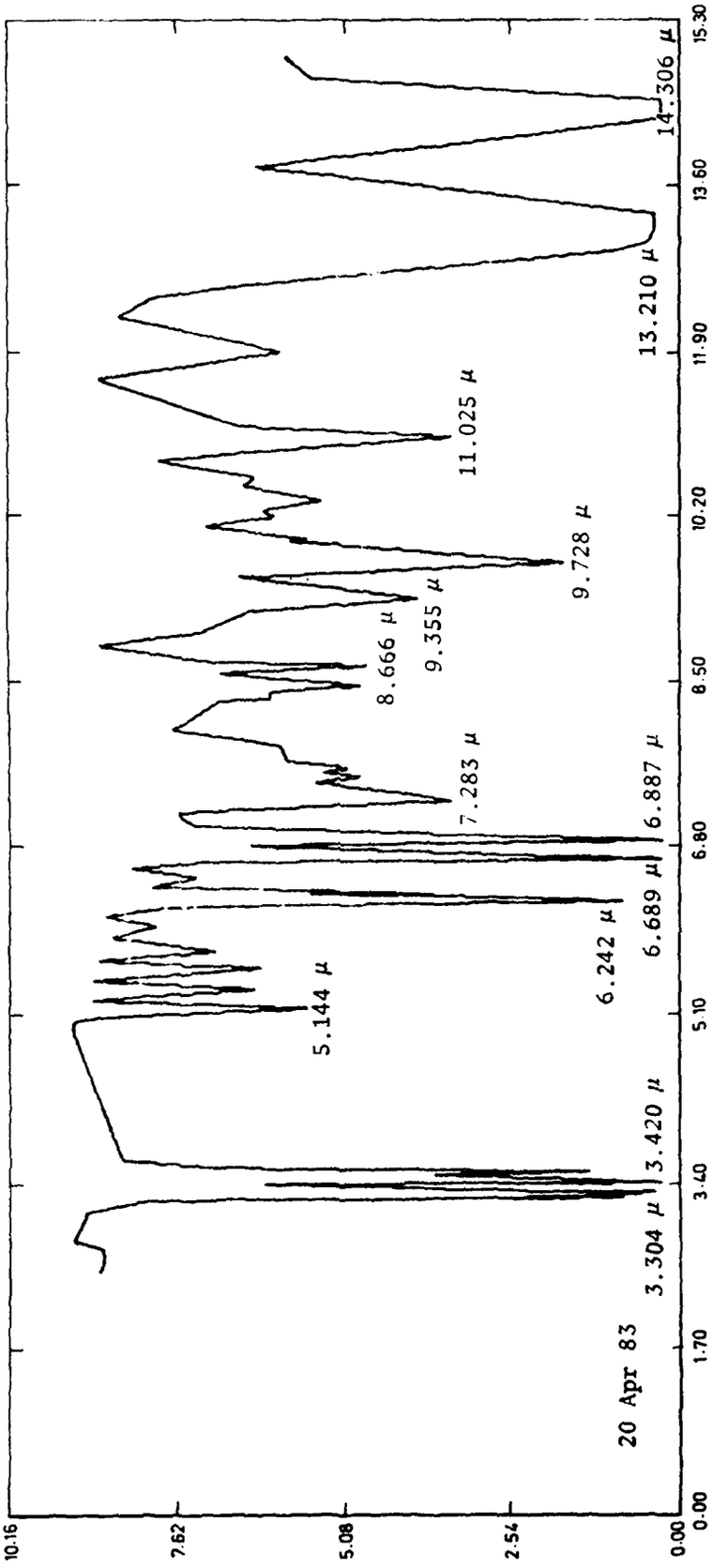

Figure 10(a). Manufacturer's data for polystyrene sample

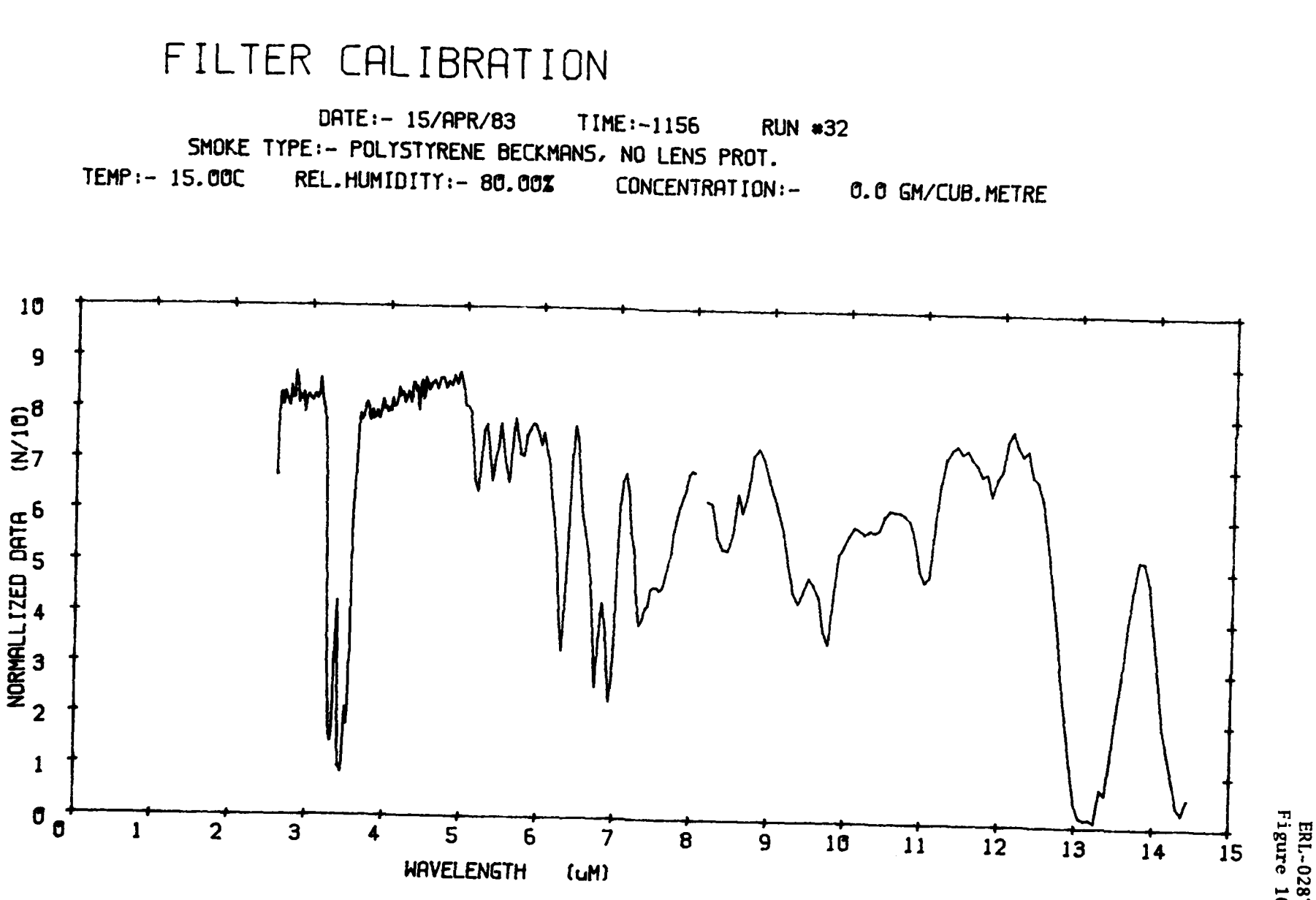

Figure 10(b). Polystyrene transmission (measured)

ERL-0287-TM
Figure 10(b)

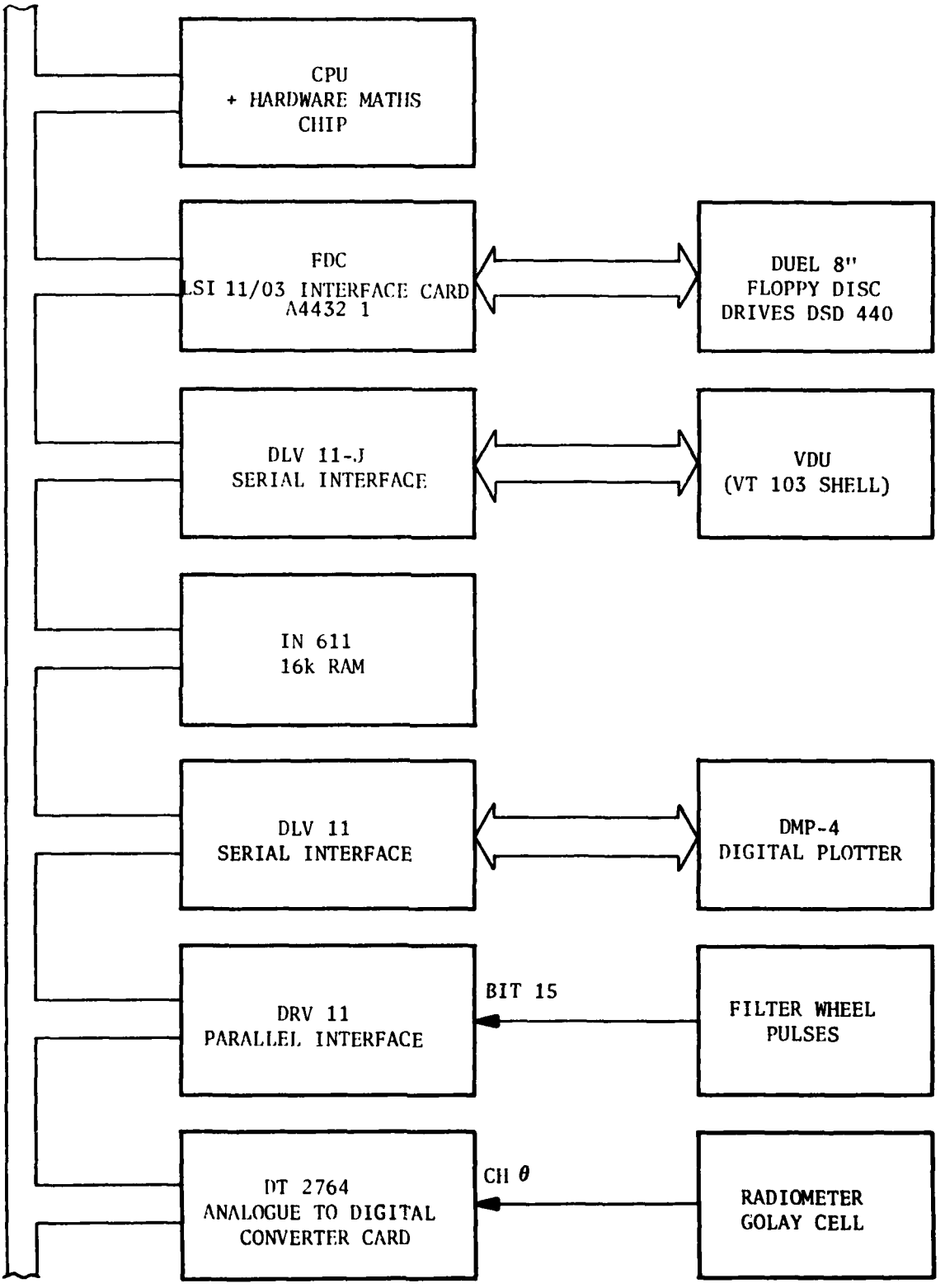

Figure 11. Data-logging/computer block diagram

DATE:- 08/OCT/82 TIME:-1121 RUN #10

SMOKE TYPE:- PHOS

TEMP:- 20.00C REL.HUMIDITY:- 65.00% CONCENTRATION:-0.1914GM/CUB.METRE

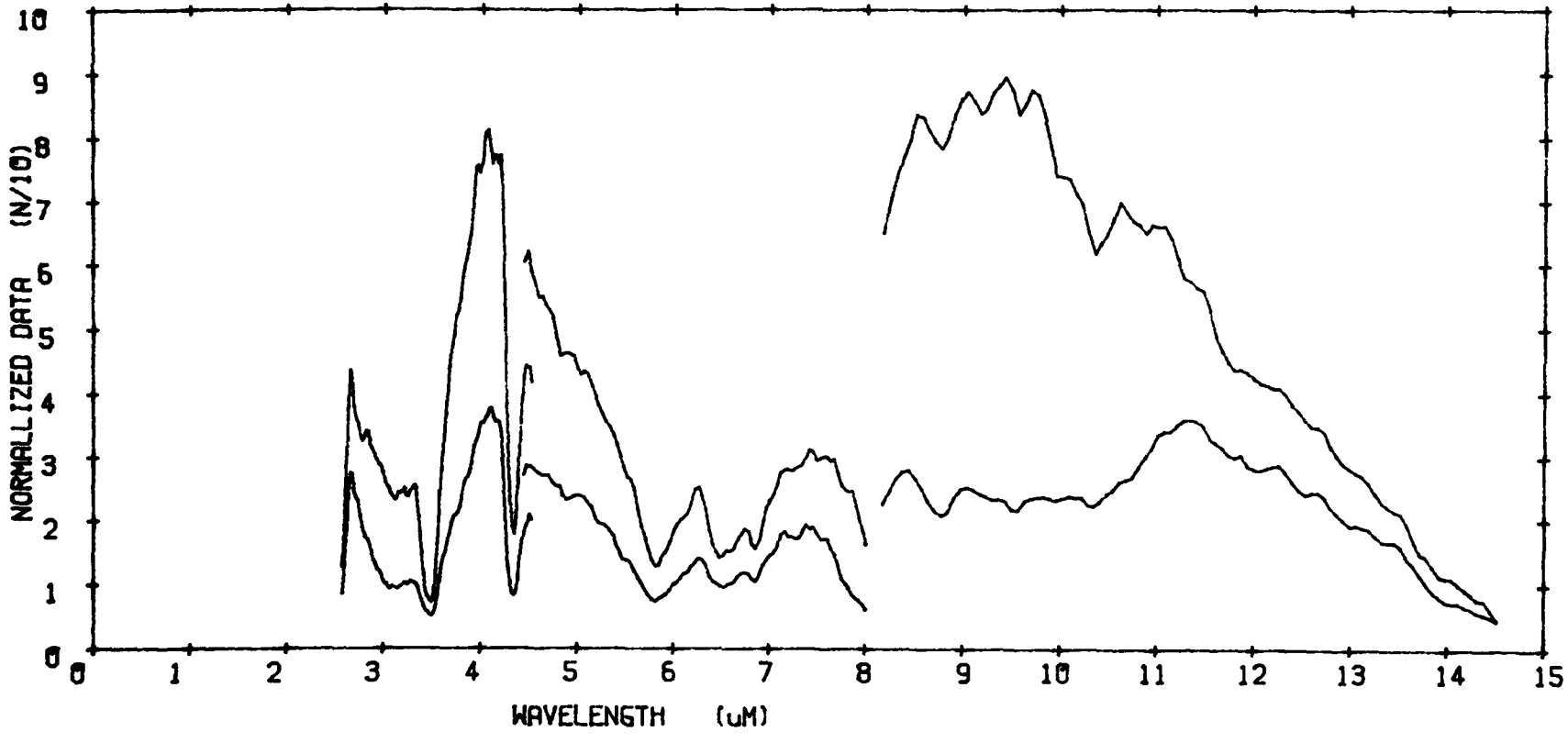

Figure 12. Sample plot of 'raw' data

ERL-0287-TM
Figure 12

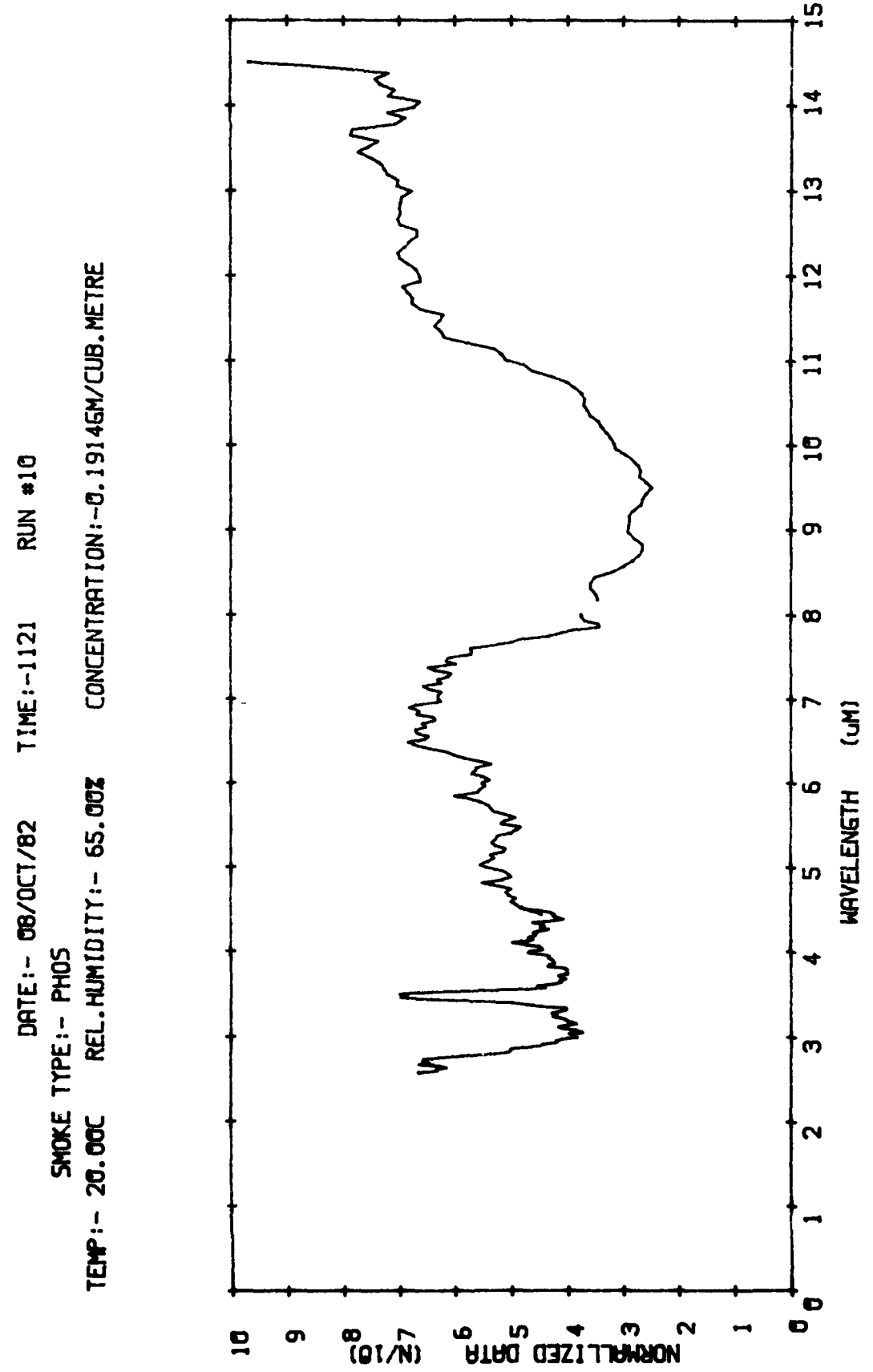

Figure 13. Sample plot of transmission

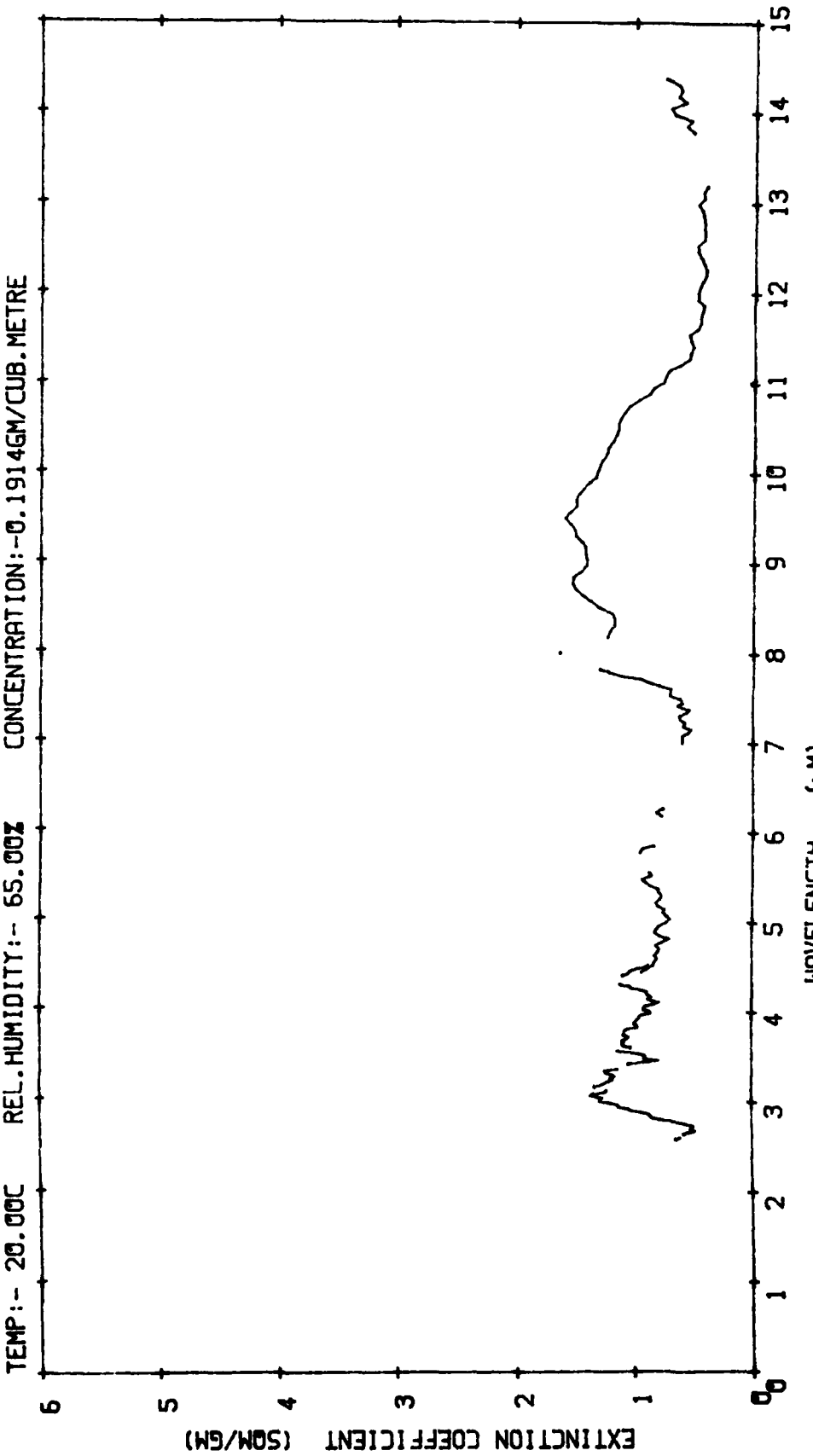

Figure 14. Sample plot of extinction coefficient

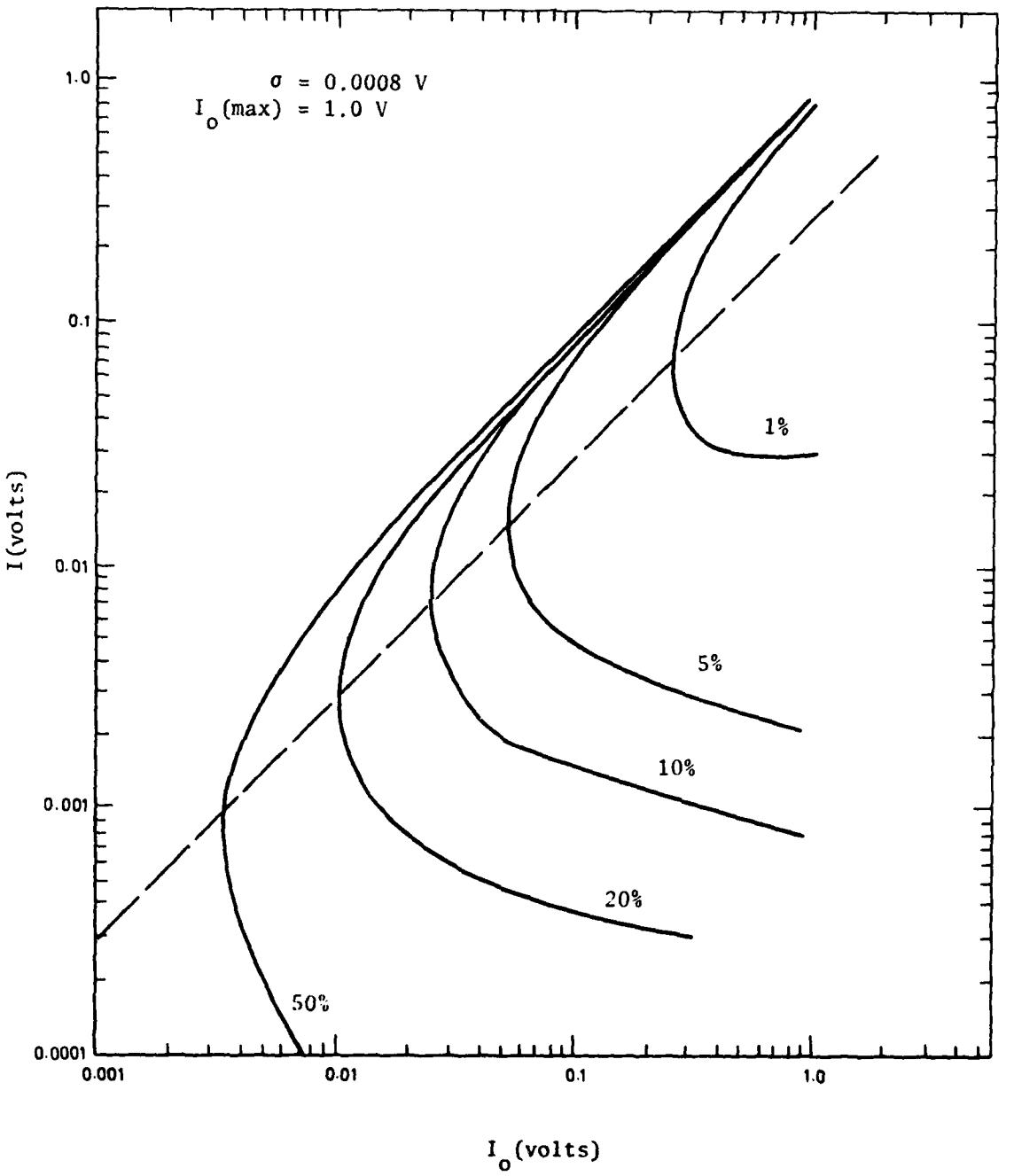

Figure 15. Contours of error in α(%) as a function of the measured signals $I_{o\lambda}$(clean air) and I_λ(obscurant)

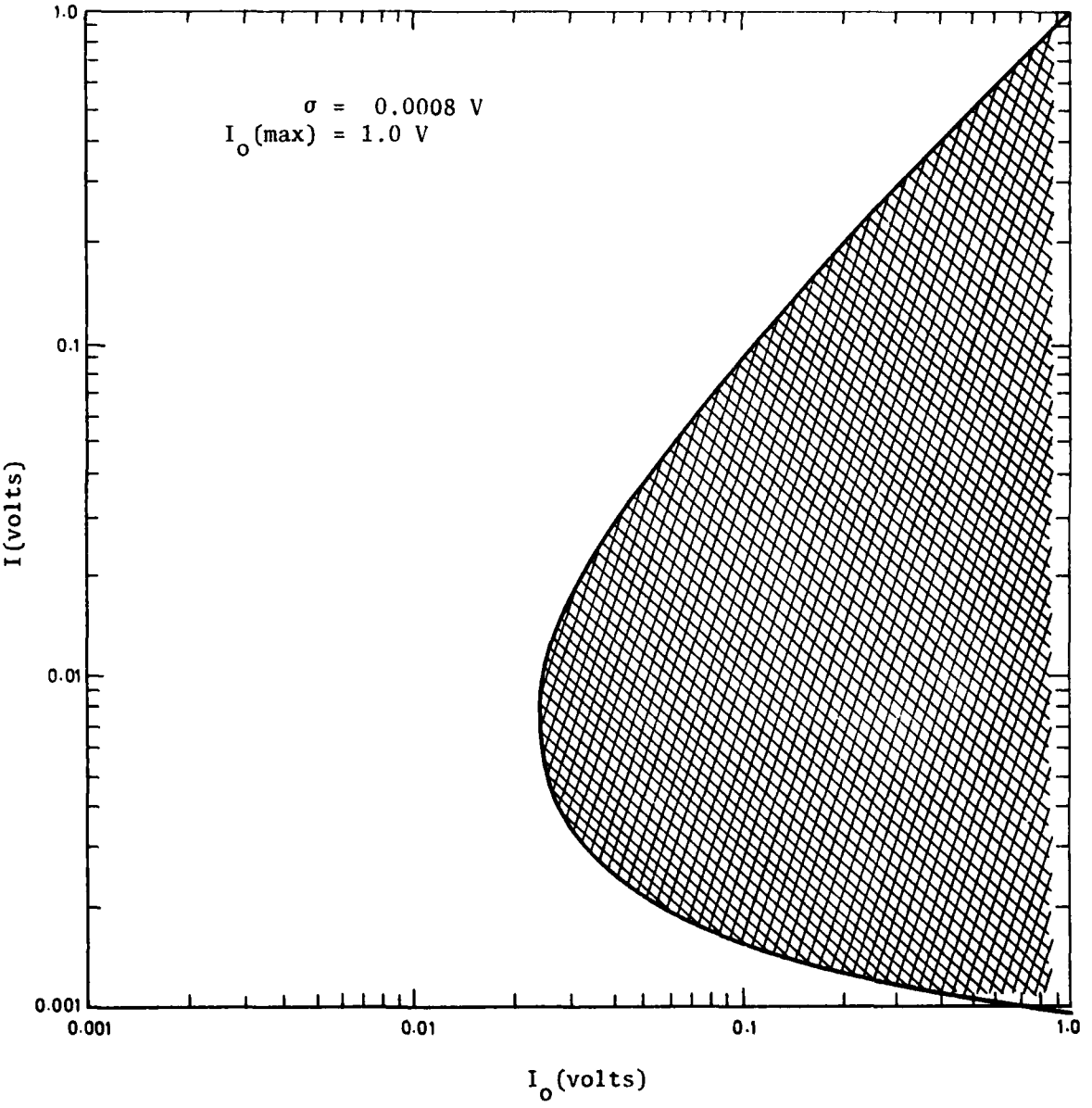

Figure 16. Permissible region for values of $I_{o\lambda}$ and I_λ to maintain the error in α to within 10%

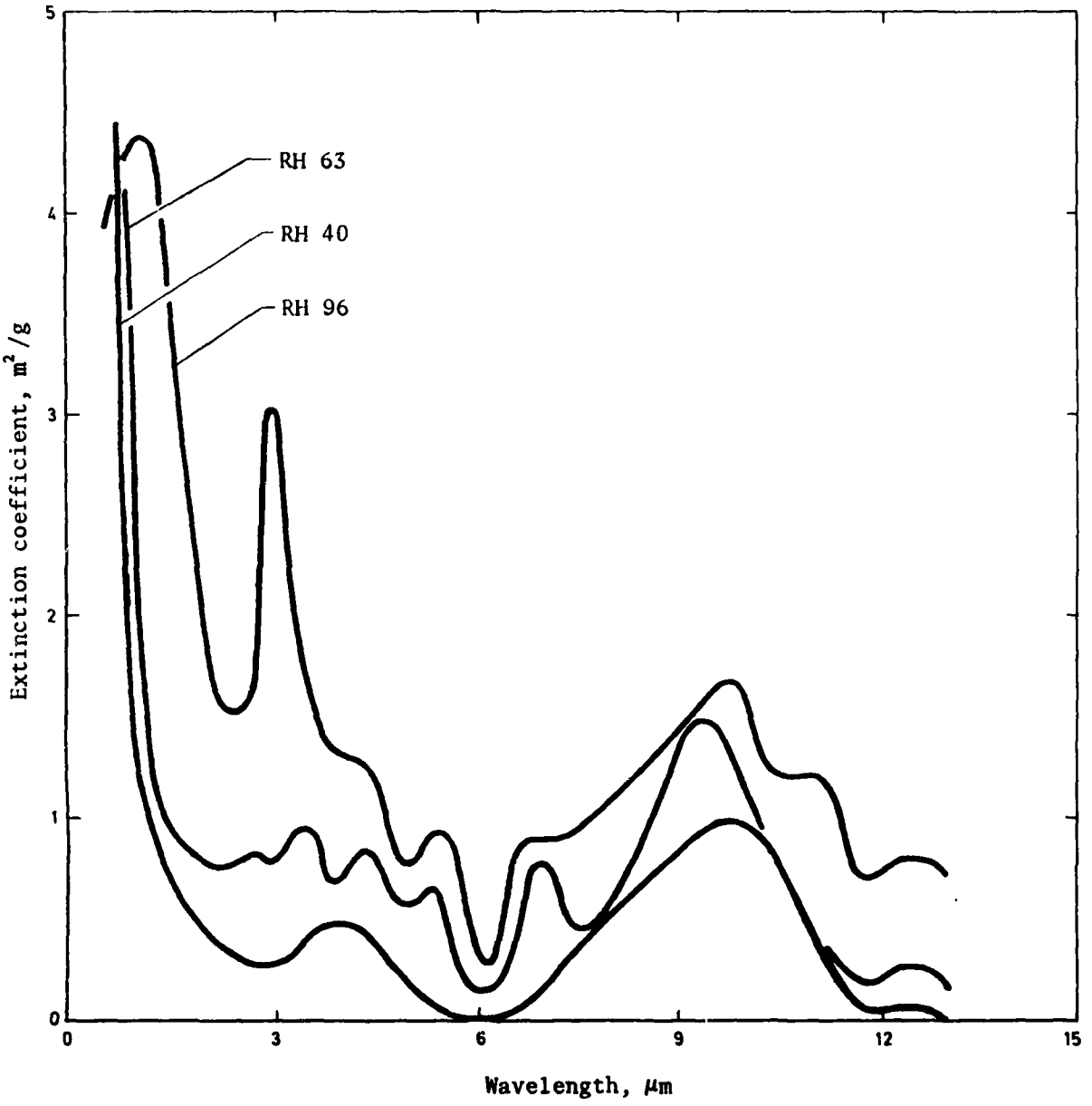

Figure 17. Extinction coefficient of red phosphorus

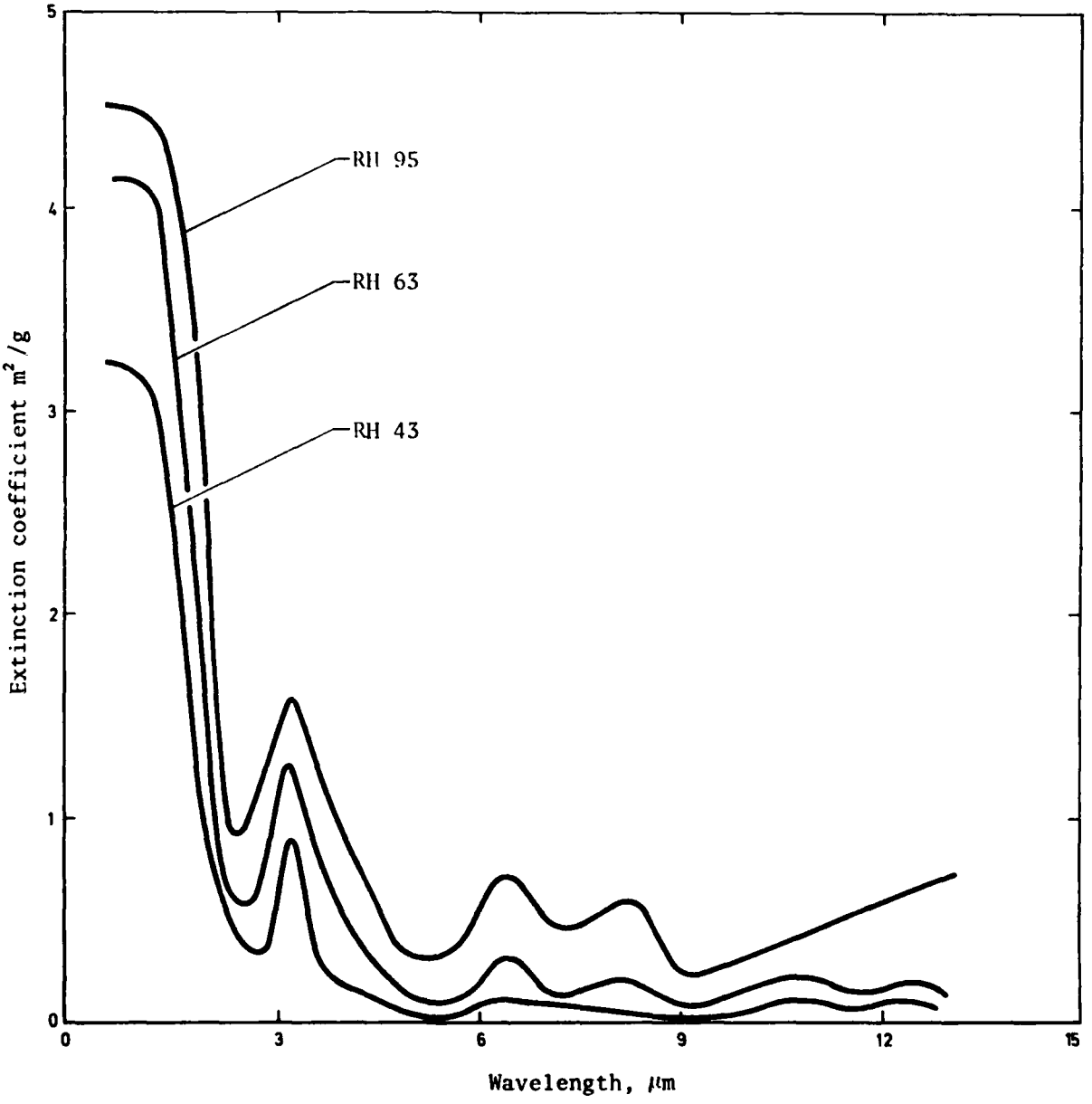

Figure 18. Extinction coefficient of hexachloroethane

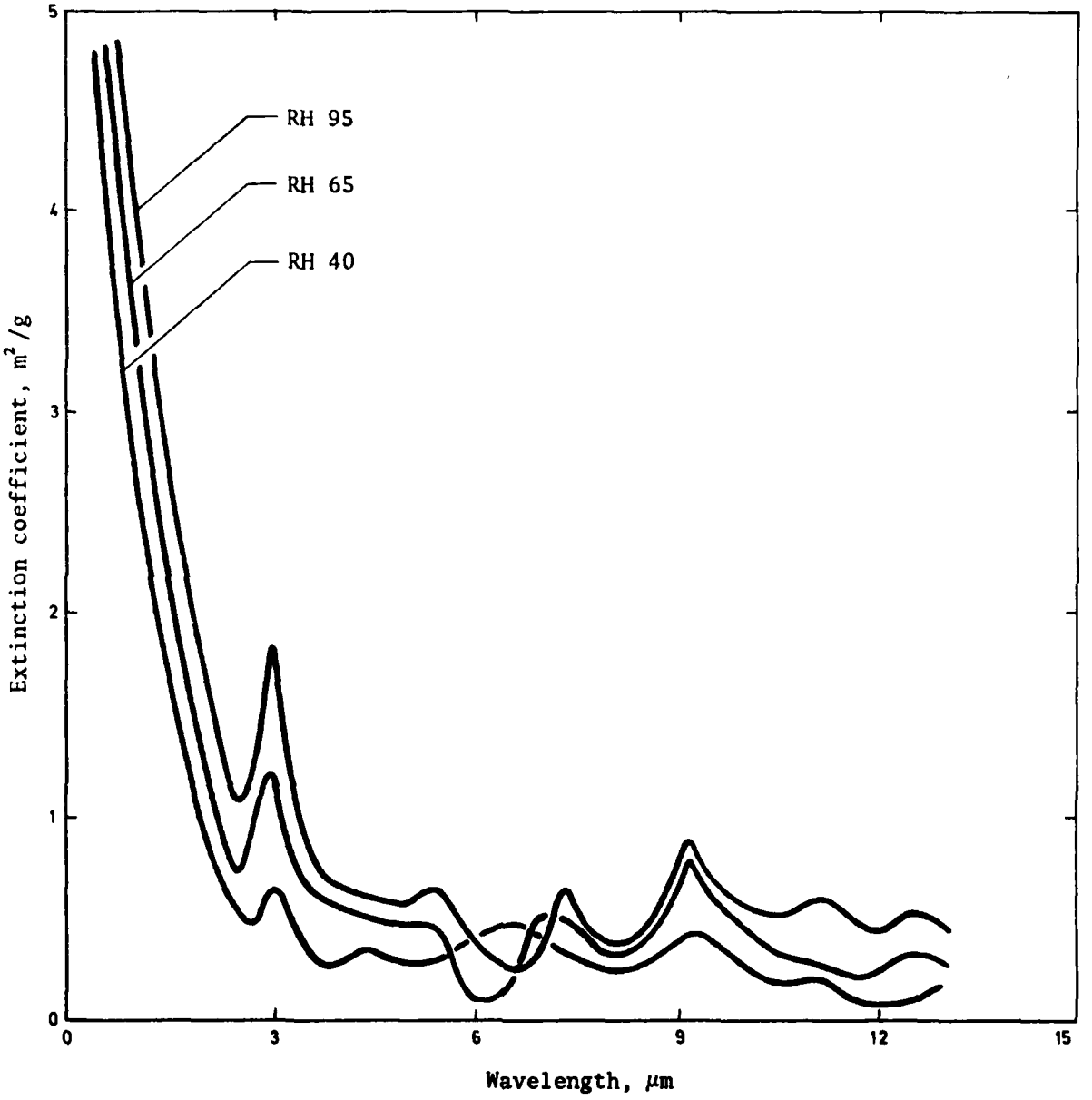

Figure 19. Extinction coefficient of oleum

DISTRIBUTION

Copy No.

EXTERNAL

In United Kingdom

Defence Science Representative, London	Title page
British Lending Library Division, Boston Spa, Yorks	1

In United States of America

Counsellor, Defence Science, Washington	Title page
Engineering Societies Library, New York, NY	2

In Australia

Department of Defence

Chief Defence Scientist	3
Deputy Chief Defence Scientist	
Controller, Projects and Analytical Studies	
Superintendent, Science and Technology Programmes	
Superintendent, Analytical Studies	4
Director, Joint Intelligence Organisation	5
Director, Materials Research Laboratories	6
Superintendent, Physical Chemistry Division, Materials Research Laboratories	7
Mr J. Bentley, Materials Research Laboratories	8
Mr R. Bird, Materials Research Laboratories	9
Mr R. Hancox, Materials Research Laboratories	10
Mr L. Redman, Materials Research Laboratories	11
Navy Scientific Adviser	12
Air Force Scientific Adviser	13
Scientific Adviser - Army	14 - 15
Director of Operations - Army	16
Director of Operational Requirements - Army	17
Director General of Logistic Development and Plans - Army	18

Document Exchange Centre
Defence Information Services Branch for:

Microfilming	19
United Kingdom, Defence Research Information Centre (DRIC)	20 - 21
United States, Defence Technical Information Centre	22 - 33
Canada, Director Scientific Information Services	34
New Zealand, Ministry of Defence	35
National Library of Australia	36

Director General, Army Development (NSO), Russell Offices
for ABCA Standardisation Officers

UK ABCA representative, Canberra	37
US ABCA representative, Canberra	38
Canada ABCA representative, Canberra	39
NZ ABCA representative, Canberra	40
Defence Library, Campbell Park	41
Library, Materials Research Laboratories	42
Library, Aeronautical Research Laboratories	43
Library, H block, Victoria Barracks, Melbourne	44
Library, RAN Research Laboratory	45

Department of Defence Support

Deputy Secretary A	46
Deputy Secretary B	
Controller, Aircraft Guided Weapons and Electronic Supply	
Controller, Munitions Supply	
Library, DDS Central Office	47
Director, Industry Development, Regional Office, Adelaide	Title page

WITHIN DRCS

Director, Electronics Research Laboratory	48
Director, Weapons Systems Research Laboratory	49
Superintendent, Electronic Warfare Division	50
Superintendent, Optoelectronics Division	51

DOCUMENT CONTROL DATA SHEET

Security classification of this page: UNCLASSIFIED

1 DOCUMENT NUMBERS

AR Number: AR-003-697

Series Number: ERL-0287-TM

Other Numbers:

2 SECURITY CLASSIFICATION

a. Complete Document: Unclassified

b. Title in Isolation: Unclassified

c. Summary in Isolation: Unclassified

3 TITLE

A LABORATORY FACILITY FOR THE MEASUREMENT OF THE OPTICAL PROPERTIES OF OBSCURANTS

4 PERSONAL AUTHOR(S):

D.J. Gambling, F.R. Dale, O.S. Scott and J. Bentley

5 DOCUMENT DATE:

August 1983

6 6.1 TOTAL NUMBER OF PAGES 32

6.2 NUMBER OF REFERENCES: 3

7 7.1 CORPORATE AUTHOR(S):

Electronics Research Laboratory

7.2 DOCUMENT SERIES AND NUMBER

Electronics Research Laboratory 0287-TM

8 REFERENCE NUMBERS

a. Task: ARM 80/175

b. Sponsoring Agency:

9 COST CODE:

333 689

10 IMPRINT (Publishing organisation)

Defence Research Centre Salisbury

11 COMPUTER PROGRAM(S) (Title(s) and language(s))

12 RELEASE LIMITATIONS (of the document):

Approved for Public Release

Security classification of this page: UNCLASSIFIED

Security classification of this page: UNCLASSIFIED

13 ANNOUNCEMENT LIMITATIONS (of the information on these pages):

No limitation

14 DESCRIPTORS:

a. EJC Thesaurus Terms

Laboratory equipment
Test facilities
Optical properties
Electrooptics
Performance evaluation

b. Non-Thesaurus Terms

Obscurants

15 COSATI CODES:

14020

16 SUMMARY OR ABSTRACT:
(if this is security classified, the announcement of this report will be similarly classified)

The presence of natural and vehicle-made dusts, fires and smoke obscurants seriously degrades the performance of electro-optical sensors operated in military environments.

This memorandum describes a laboratory facility for the measurement of the visual and infrared mass extinction coefficients of obscurants under controlled environmental conditions.

Security classification of this page: UNCLASSIFIED